Bioconjugate Chemistry

Communication

pubs.acs.org/bc

Antibody Modified Gold Nanoparticles for Fast and Selective, Colorimetric T7 Bacteriophage Detection

Adam Lesniewski,*[,†] Marcin Los,[†,‡] Martin Jonsson-Niedziółka,[†] Anna Krajewska,[‡] Katarzyna Szot,[†,‡] Joanna M. Los,[‡] and Joanna Niedziolka-Jonsson*[,†]

[†]Institute of Physical Chemistry, Polish Academy of Sciences, Kasprzaka 44/52, 01-224 Warszawa, Poland

[‡]Department of Molecular Biology, University of Gdansk, Wita Stwosza 59, 80-308 Gdansk, Poland

Supporting Information

ABSTRACT: Herein, we report a colorimetric immunosensor for T7 bacteriophage based on gold nanoparticles modified with covalently bonded anti-T7 antibodies. The new immunosensor allows for a fast, simple, and selective detection of T7 virus. T7 virions form immunological complexes with the antibody modified gold nanoparticles which causes them to aggregate. The aggregation can be observed with the naked eye as a color change from red to purple, as well as with a UV−vis spectrophotometer. The aggregate formation was confirmed with SEM imaging. Sensor selectivity against the M13 bacteriophage was demonstrated. The limit of detection (LOD) is 1.08 × 10^{10} PFU/mL (18 pM) T7. The new method was compared with a traditional plaque test. In contrast to biological tests the colorimetric method allows for detection of all T7 phages, not only those biologically active. This includes phage ghosts and fragments of virions. T7 virus has been chosen as a model organism for adenoviruses. The described method has several advantages over the traditional ones. It is much faster than a standard plaque test. It is more robust since no bacteria−virus interactions are utilized in the detection process. Since antibodies are available for a large variety of pathogenic viruses, the described concept is very flexible and can be adapted to detect many different viruses, not only bacteriophages. Contrary to the classical immunoassays, it is a one-step detection method, and no additional amplification, e.g., enzymatic, is needed to read the result.

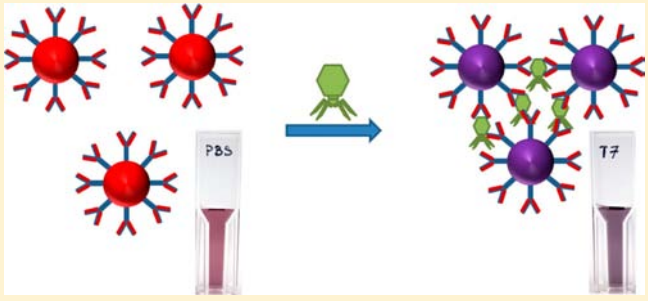

INTRODUCTION

Viruses are small infectious agents responsible for a great variety of diseases that oppress mankind. Examples of viral diseases are hepatitis, HSV-1 and HSV-2 infection, mononucleosis, AIDS, influenza, pneumonia, measles, mumps, SARS, Ebola, Machupo, and many others. An important group of pathogenic viruses are adenoviruses causing respiratory illness, gastroenteritis, conjunctivitis, and cystitis. To be able to order a proper medical treatment, a quick and unequivocal diagnosis is essential.

In the case of assays aimed at detecting whole viruses, the most sensitive are biological assays, which, in some bacteriophages, are able to detect even a single phage particle. The detection assays in the case of phages usually utilize the infection of a liquid culture of host bacterial cells or the double agar layer method (infection in agar), or a combination of both. The output is the lysis of the bacterial culture or plaque formation on the double agar layer plates, which indicates phage presence.[1] However, the test is generic and phages cannot be fully identified using this method. Both methods, but especially the liquid culture method, are prone to yielding false negatives. The time required for the assay to be completed varies greatly and depends on the host and the particular phage. It may show results within 2−48 h in the case of fast-growing bacteria like, e.g., *Escherichia coli*. In the case of mammalian viruses, including human pathogens, biological methods are not always possible, and usually their sensitivity, with some exceptions, is relatively low. Biological assays, moreover, often require clean samples, skilled personnel, and are usually labor intensive. The high risk of false positives and false negatives associated with these assays increases the interest in alternative approaches to diagnostics. Use of antibodies, due to their very specific antigen recognition, allows for selective detection of virus regardless of other components of the sample. As the binding constant in assays depends almost entirely on the affinity and avidity of the antibody, the easiest way to increase test sensitivity is the improvement in the detection of a signal that indicates a binding event. In automated or semiautomated assays utilizing antibodies, various approaches are employed, the majority of which use secondary antibodies and systems of signal amplification which result in significant increase of the sensitivity. For example, Los et al. were able to detect ∼10^7 PFU/mL.[2] However, signal amplification methods also may yield false negatives. Additionally, they increase the sample

Received: January 25, 2014
Revised: March 26, 2014
Published: March 28, 2014

dx.doi.org/10.1021/bc500035y | *Bioconjugate Chem.* 2014, 25, 644−648

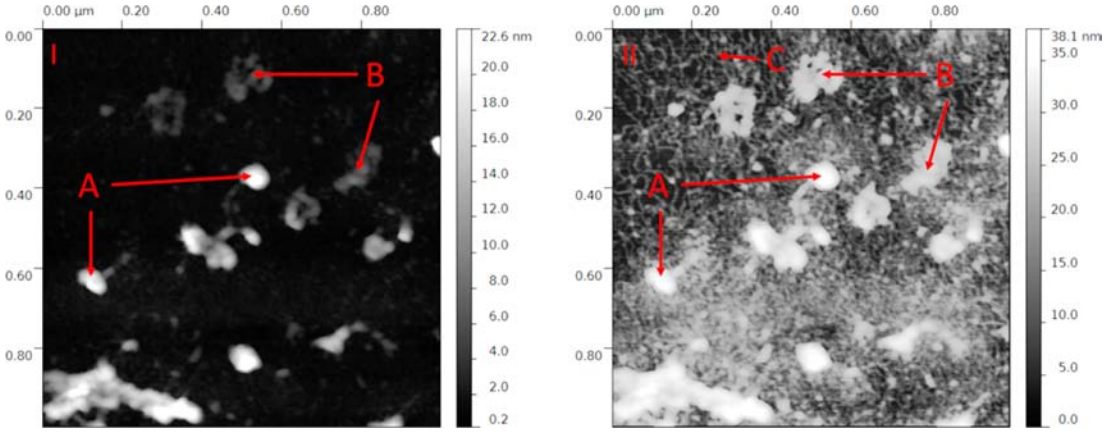

Figure 1. AFM images of T7 bacteriophages on mica (I) linear *Z* scale, (II) nonlinear *Z* scale: (A) complete phages, (B) phage fragments/ghosts, and (C) DNA strands.

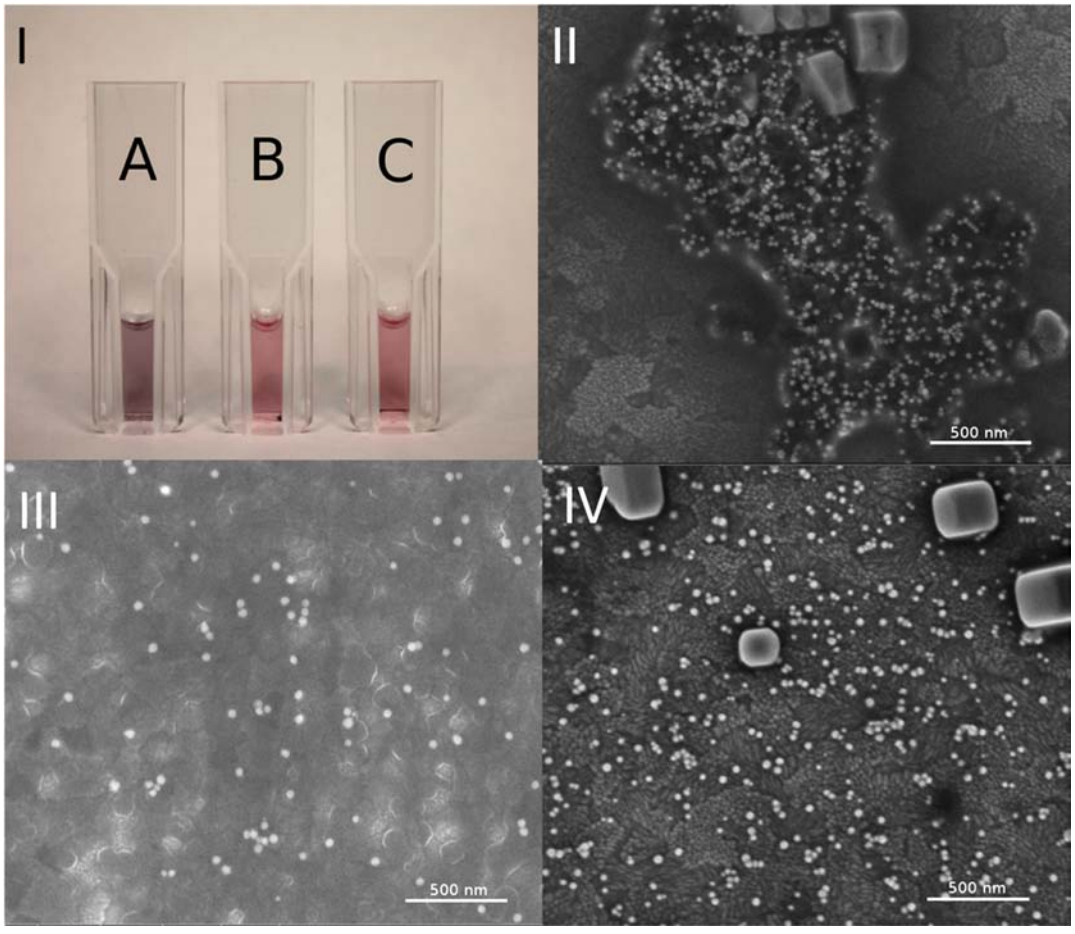

Figure 2. (IA) AuNPs-Cys-IgGanti-T7 with 16.5 μL of 4.8×10^{12} PFU/mL T7, (IB) 16.5 μL of 4.8×10^{12} PFU/mL M13, and (IC) 16.5 μL of PBS addition. SEM images of AuNPs-Cys-IgGanti-T7 after (II) T7, (III) M13, and (IV) PBS addition.

analysis time. Therefore, label-free measurements are being more widely employed. Methods based on quartz crystal microbalance[3] and impedance measurements[4] have already been shown to be successful in detection of small virus quantities, but still there is a need for cheap assays using parameters easier to measure, like, e.g., absorbance.

The T7 bacteriophage is an excellent model organism for developing new virus detection methods. The T7 belongs to the *Podoviridae* phage family. The structure and morphology of this virus is very similar to the adenoviruses.[5] Both belong to the category of non-enveloped viruses. Their sizes are 55 nm and ~70−100 nm for T7[6] and adenoviruses,[7] respectively. The T7 virus does not possess the spikes characteristic of adenoviruses but instead has fibers on its tail. T7's tail is short and does not contribute much to the mass of the virion (Figure 1). It is noncontagious for humans, animals, and plants and is easy to produce and quantify and is stable in solution.

In recent years, gold nanoparticles (AuNPs) have commonly been used as transducers in biosensing devices.[8,9] The localized surface plasmon resonance (LSPR) of AuNPs is utilized to

dx.doi.org/10.1021/bc500035y | *Bioconjugate Chem.* 2014, 25, 644−648

transform the biochemical signal into an optical one. It is well-known that the LSPR peak position is dependent on the size and shape of the nanoparticles, as well as on the dielectric constant of the environment. It was previously demonstrated that changing the interparticle distance radically changes the AuNPs' LSPR peak position.[10] Well-dispersed ca. 30-nm-diameter AuNPs show a maximum absorption at ca. 520 nm. Once they start forming aggregates, the absorption band shifts to ca. 600−800 nm. This significant change in peak absorption can be easily observed with the naked eye as well as measured quantitatively with a UV−vis spectrophotometer. This phenomenon has already been used for sensing of various analytes such as Hg^{2+} ions (LOD = 100 nM);[11,12] various proteins (LOD = 10 nM and 25 nM);[13] melamine (LOD = 6×10^{-6} g/L);[14] cancer cells;[15] endonuclease activity and inhibition;[16] nitrite (LOD = 21.7 μM);[17] cysteine (LOD = 100 nM);[18] and influenza virus (LOD = 0.156 vol %).[19]

Immunosensors are an important group of biosensors based on the detection of antigen−antibody complex formation.[20] In this paper a new T7 bacteriophage immunosensor is described. To the best of our knowledge this is the first time where antibody modified gold nanoparticles were used for colorimetric virus detection. Cysteamine stabilized gold nanoparticles (AuNPs-Cys) covalently modified with anti-T7 antibody (AuNPs-Cys-IgGanti-T7) aggregate in the presence of T7 virions. No aggregation was observed if M13 solution or PBS was introduced to the system, instead of T7 bacteriophages solution, suggesting that specific antigen−antibody interaction is responsible for AuNPs-Cys-IgGanti-T7 aggregation. The described system allows detecting T7 phages in low concentration, from 1.08×10^{10} PFU/mL (18 pM). A linear signal increase was observed up to at least 4.8×10^{10} PFU/mL T7 concentration. The described method is faster than classic determination methods such as plaque test[21] or immunoassays. Moreover, there is no need for additional signal amplification. Since the method is based on the antibody−antigen interaction there is no need for the viruses to be biologically active. One can detect bacteriophage ghosts as well as full phages. This fact makes the described strategy promising for quick, reliable, and cost-effective detection of nonbacteriophage viruses that do not interact with bacteria.

RESULTS AND DISCUSSION

Small aliquots of 4.8×10^{12} PFU/mL T7 solution were added to 0.5 mL of as-synthesized AuNPs-Cys-IgGanti-T7 (see details in Supporting Information). To check the selectivity of the system the same amounts of 4.8×10^{12} PFU/mL M13 were added to the fresh suspension of AuNPs-Cys-IgGanti-T7. A control experiment, where only PBS was added to the system, was conducted.

In the case of T7 phage addition, an immediate change of color from pink to purple was observed (Figure 2I A), whereas no change was observed in the case of M13 and PBS addition (Figure 2I B and C). This change was also clearly visible in the UV−vis spectrum. After the T7 addition a decrease of the characteristic AuNPs-Cys-IgGanti-T7 LSPR peak at ca. 520 nm was observed (Figure 3II). This phenomenon is due to two main processes. First, adding T7 solution to the AuNPs-Cys-IgGanti-T7 suspension causes its dilution, which lowers the absorbance. This phenomenon was also observed when 10 μL of PBS was added to the AuNPs-Cys-IgGanti-T7 instead of T7 (not shown). However, the effect was more pronounced in the case of T7 addition. Thus, a second process causes the decrease

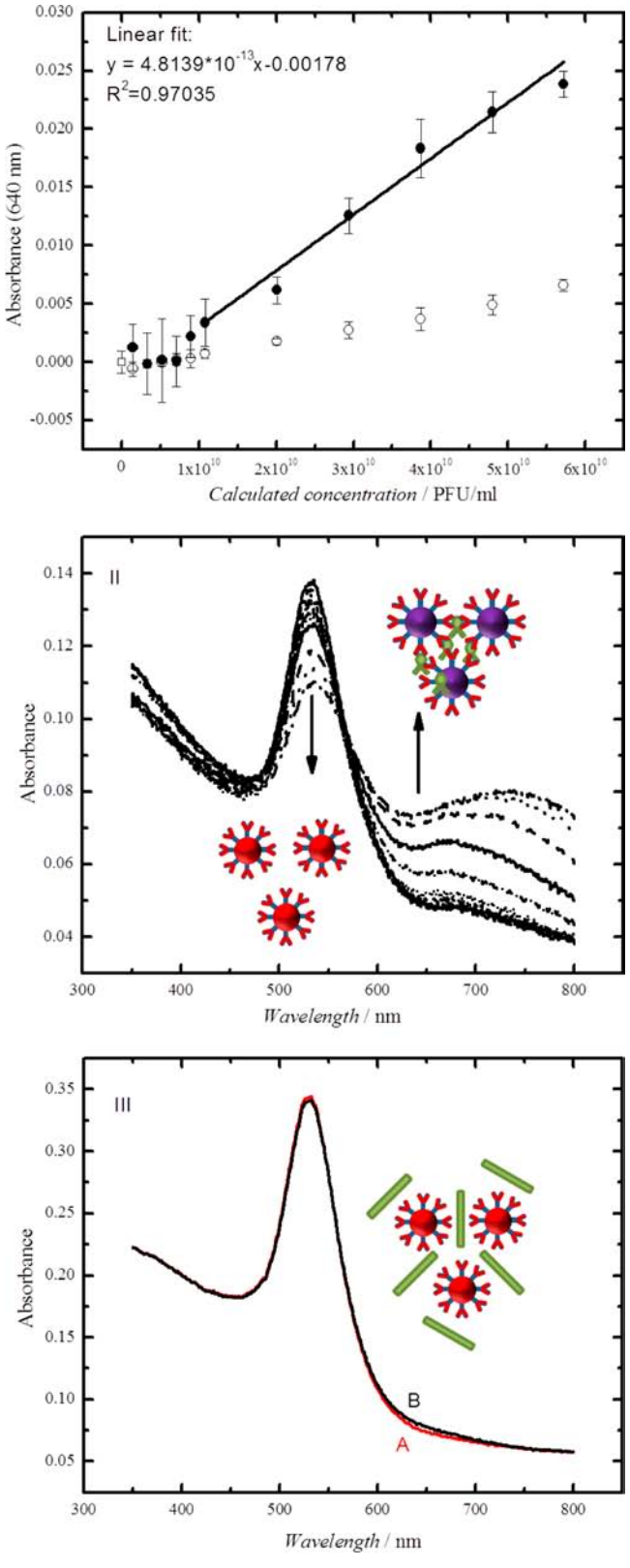

Figure 3. I. Calibration curves for AuNPs-Cys-IgGanti-T7 after addition of T7 (●) and M13 (○) solutions. (□) is the background without added virus. Error bars represent SD with n = 3. II. Absorbance spectra for AuNPs-Cys-IgGanti-T7 with T7 solutions added. T7 concentration increase marked with arrows. III. Absorbance spectra for AuNPs-Cys-IgGanti-T7 with 1.08×10^{10} PFU/mL of T7 (A) and 3.87×10^{10} PFU/mL M13 added (B).

dx.doi.org/10.1021/bc500035y | Bioconjugate Chem. 2014, 25, 644−648

of the 520 nm peak and the change in color. This is the appearance of a peak at ca. 600−800 nm related to the aggregated AuNPs (Figure 3II).

These results were confirmed by scanning electron microscopy. Aliquots of AuNPs-Cys-IgGanti-T7 with T7, M13, or PBS added were dropped onto ITO glass. After solvent evaporation, the glass slides were investigated with SEM (Figure 2II,III,IV). It is clearly seen that after T7 addition gold nanoparticles form aggregates bound together with organic material (Figure 2II). Almost no aggregation was observed if M13 phage solution was added to the system instead of T7 (Figure 2III), nor was aggregation observed for the PBS buffer alone (Figure 2IV).

To check the detection limit of the system 0.5 mL of AuNPs-Cys-IgGanti-T7 solution was placed in UV−vis cuvettes. Next, small aliquots of T7, M13 solutions or PBS were added to the system. After each addition a UV−vis spectrum was recorded. The spectrum recorded for clean AuNPs-Cys-IgGanti-T7 was subtracted from the subsequent scans. Absorbance changes were monitored at 520 nm (AuNPs absorption band) and 640 nm (AuNP aggregates absorption band). When the T7 solution is added to the AuNPs-Cys-IgGanti-T7, the 520 nm peak is decreasing due to dilution of the stock solution (Figure 3II). However, the peak decrease is faster than for the M13 solution and the PBS addition. The 640 nm peak was found to significantly increase when the concentration of T7 reaches 1.08×10^{10} PFU/mL (18 pM) and increases further with T7 concentration (Figure 3I, II). This is due to the AuNPs-Cys-IgGanti-T7 aggregation caused by T7 phages. Only a very small aggregation peak was observed if M13 (Figure 3I, III) solution or PBS (not shown) was added to the AuNPs-Cys-IgGanti-T7 solution. The origin of the nonzero signal for the M13 phage may be that polyclonal antibodies were used for nanoparticle modification. Probably a fraction of the antibodies can recognize some epitopes on the M13 surface. The other possibility is that the gold nanoparticles interact with the free DNA strands that are present in the phage samples. The lowest measured T7 concentration that gives the signal above three times the standard deviation of the blank sample was 1.08×10^{10} PFU/mL; therefore, this concentration is considered to be the method's LOD. Moreover, a linear relationship between absorbance growth and T7 bacteriophage concentration was observed (Figure 3I). This observation makes the system useful for qualitative as well as quantitative T7 bacteriophage detection.

The concentrations of the T7 solutions have been independently measured with the plaque test. It was found that the concentration measured by plaque test was ca. 5 times smaller than the one calculated from the T7 stock dilutions. That means that only one-fifth of the viruses retained their biological activity after the dilution process, and only they can be detected with a plaque test. One can clearly see the difference between the complete phages and the phage fragments in the AFM images (Figure 1). The DNA strands from the broken phages can also be observed (Figure 1II).

CONCLUSIONS

The study describes a new T7 phage immunosensor based on AuNPs aggregation. The developed sensor allows for qualitative and quantitative analysis of T7 phages. The LOD of the method was defined as 1.08×10^{10} PFU/mL (18 pM). The linear relationship between the analytical signal and T7 concentration was demonstrated up to 5.72×10^{10} PFU/mL (limited by the T7 stock solution). The sensor was found to be selective against M13 phage, which is an advantage over the plaque assay. This is possible because, unlike in plaque tests, there were no bacteria−virus interactions utilized in the detection process. The new method is based on antibody−antigen interaction, so contrary to the plaque assay, there is no need for detected viruses to be biologically active. It is possible to detect phage ghosts and bacteriophage fragments. It is important to emphasize the high precision of the method. Results can be obtained in a short time in a one-step procedure. There is no need for the multistep procedure used in traditional immunoassay approach.

ASSOCIATED CONTENT

Supporting Information

Bacteriophage production and nanoparticle synthesis and characterization. This material is available free of charge via the Internet at http://pubs.acs.org/.

AUTHOR INFORMATION

Corresponding Authors

*E-mail: alesniewski@ichf.edu.pl.

*E-mail: joaniek@ichf.edu.pl. Tel: +48 22 343 31 30, fax: +48 22 343 33 33.

Notes

The authors declare no competing financial interest.

ACKNOWLEDGMENTS

This work was supported by the Foundation for Polish Science through the FOCUS Programme no F3/2010/P/2013. Access to SEM was funded by the EC 7.FP under the Research Potential (Coordination and Support Actions FP7-REGPOT-CT-2011-285949-NOBLESSE).

REFERENCES

(1) Sambrook, J., Fritsh, E. F., and Maniatis, T. (1989) *Molecular cloning: A laboratory manual*, 2nd ed., Cold Spring Harbor Laboratory Press, Cold Spring Harbor, NY.

(2) Łoś, M., Łoś, J. M., Blohm, L., Spillner, E., Grunwald, T., Albers, J., Hintsche, R., and Wegrzyn, G. (2005) Rapid detection of viruses using electrical biochips and anti-virion sera. *Lett. Appl. Microbiol. 40*, 479−85.

(3) Wang, R., and Li, Y. (2013) Hydrogel based QCM aptasensor for detection of avian influenza virus. *Biosens. Bioelectron. 42*, 148−55.

(4) Lum, J., Wang, R., Lassiter, K., Srinivasan, B., Abi-Ghanem, D., Berghman, L., Hargis, B., Tung, S., Lu, H., and Li, Y. (2012) Rapid detection of avian influenza H5N1 virus using impedance measurement of immuno-reaction coupled with RBC amplification. *Biosens. Bioelectron. 38*, 67−73.

(5) Roberts, M., White, J., Grutter, M., and Burnett, R. (1986) Three-dimensional structure of the adenovirus major coat protein hexon. *Science (Washington, DC, U.S.) 232*, 1148−1151.

(6) Serwer, P. (1977) Flattening and shrinkage of bacteriophage T7 after preparation for electron microscopy by negative staining. *J. Ultrastruct. Res. 58*, 235−243.

(7) Kennedy, M. A., and Parks, R. J. (2009) Adenovirus virion stability and the viral genome: size matters. *Mol. Ther. 17*, 1664−6.

(8) Saha, K., Agasti, S. S., Kim, C., Li, X., and Rotello, V. M. (2012) Gold nanoparticles in chemical and biological sensing. *Chem. Rev. 112*, 2739−79.

(9) Zeng, S., Yong, K.-T., Roy, I., Dinh, X.-Q., Yu, X., and Luan, F. (2011) A review on functionalized gold nanoparticles for biosensing applications. *Plasmonics 6*, 491−506.

(10) Rechberger, W., Hohenau, A., Leitner, A., Krenn, J. R., Lamprecht, B., and Aussenegg, F. R. (2003) Optical properties of two interacting gold nanoparticles. *Opt. Commun. 220*, 137−141.
(11) Huang, C.-C., and Chang, H.-T. (2007) Parameters for selective colorimetric sensing of mercury(II) in aqueous solutions using mercaptopropionic acid-modified gold nanoparticles. *Chem. Commun. (Cambridge) 43*, 1215−7.
(12) Lee, J.-S., Han, M. S., and Mirkin, C. A. (2007) Colorimetric detection of mercuric ion (Hg2+) in aqueous media using DNA-functionalized gold nanoparticles. *Angew. Chem., Int. Ed. 46*, 4093−6.
(13) Aili, D., Selegård, R., Baltzer, L., Enander, K., and Liedberg, B. (2009) Colorimetric protein sensing by controlled assembly of gold nanoparticles functionalized with synthetic receptors. *Small 5*, 2445−52.
(14) Guan, H., Yu, J., and Chi, D. (2013) Label-free colorimetric sensing of melamine based on chitosan-stabilized gold nanoparticles probes. *Food Control 32*, 35−41.
(15) El-Sayed, I. H., Huang, X., and El-Sayed, M. a. (2005) Surface plasmon resonance scattering and absorption of anti-EGFR antibody conjugated gold nanoparticles in cancer diagnostics: applications in oral cancer. *Nano Lett. 5*, 829−34.
(16) Xu, X., Han, M. S., and Mirkin, C. A. (2007) A gold-nanoparticle-based real-time colorimetric screening method for endonuclease activity and inhibition. *Angew. Chem., Int. Ed. 46*, 3468−70.
(17) Daniel, W. L., Han, M. S., Lee, J.-S., and Mirkin, C. A. (2009) Colorimetric nitrite and nitrate detection with gold nanoparticle probes and kinetic end points. *J. Am. Chem. Soc. 131*, 6362−3.
(18) Lee, J.-S., Ulmann, P. A., Han, M. S., and Mirkin, C. A. (2008) A DNA-gold nanoparticle-based colorimetric competition assay for the detection of cysteine. *Nano Lett. 8*, 529−33.
(19) Lee, C., Gaston, M. A., Weiss, A. A., and Zhang, P. (2013) Colorimetric viral detection based on sialic acid stabilized gold nanoparticles. *Biosens. Bioelectron. 42*, 236−41.
(20) Holford, T. R. J., Davis, F., and Higson, S. P. J. (2012) Recent trends in antibody based sensors. *Biosens. Bioelectron. 34*, 12−24.
(21) Anderson, B., Rashid, M. H., Carter, C., Pasternack, G., Rajanna, C., Revazishvili, T., Dean, T., Senecal, A., and Sulakvelidze, A. (2011) Enumeration of bacteriophage particles: Comparative analysis of the traditional plaque assay and real-time QPCR- and nanosight-based assays. *Bacteriophage 1*, 86−93.